

Ancient stars beyond the Local Group: RR Lyrae variables and Blue Horizontal Branch stars in Sculptor Group Dwarf Galaxies¹

G. S. Da Costa¹, M. Rejkuba², H. Jerjen¹ and E. K. Grebel³

ABSTRACT

We have used *Hubble Space Telescope* ACS images to generate color-magnitude diagrams that reach below the magnitude of the horizontal branch in the Sculptor Group dwarf galaxies ESO294-010 and ESO410-005. In both diagrams blue horizontal branch stars are unambiguously present, a signature of the existence of an ancient stellar population whose age is comparable to that of the Galactic halo globular clusters. The result is reinforced by the discovery of numerous RR Lyrae variables in both galaxies. The occurrence of these stars is the first direct confirmation of the existence of ancient stellar populations beyond the Local Group and indicates that star formation can occur at the earliest epochs even in low density environments.

Subject headings: galaxies: dwarf — galaxies: individual (ESO 294-010, ESO 410-005) — galaxies: stellar content — stars: horizontal-branch — stars: variables: other

1. Introduction

In 1938 Shapley reported the discovery of a stellar system of previously unknown type in the constellation of Sculptor (Shapley 1938). His preferred interpretation of the system was as “a super cluster of the globular type”, an interpretation given credence by the subsequent identification of ‘cluster-type’ variables (now generally known as RR Lyrae variables) in the system by Baade & Hubble (1939). We now know this stellar system as the Sculptor dwarf spheroidal (dSph)

¹Research School of Astronomy & Astrophysics, The Australian National University, Mt Stromlo Observatory, via Cotter Rd, Weston, ACT 2611, Australia

²European Southern Observatory, Karl-Schwarzschild-Strasse 2, 85748 Garching bei Munchen, Germany

³Astronomisches Rechen-Institut, Zentrum für Astronomie der Universität Heidelberg, Mönchhofstr. 12-14, D-69120 Heidelberg, Germany

¹Based on observations made with the NASA/ESA Hubble Space Telescope, obtained at the Space Telescope Science Institute, which is operated by the Association of Universities for Research in Astronomy, Inc., under NASA contract NAS 5-26555. These observations are associated with program GO-10503.

galaxy, an example of what is perhaps the most common type of galaxy in the Universe. In the intervening 70 or more years we have learned much about the stellar populations of dSph galaxies, and have recognised that they are generally much more complex than the (relatively) simple stellar populations of globular clusters. One feature, however, is common between globular clusters and dwarf galaxies of all types, at least as far as Local Group objects is concerned. This is the existence in all dwarf galaxies where adequate data are available of a stellar population that is comparable in age to that of the Galactic halo globular clusters. In other words, while the subsequent star formation history varies strongly from dwarf to dwarf, it appears for Local Group systems at least, that star formation did occur at the earliest epochs in all systems – there are no Local Group dwarfs known to lack ancient stars (e.g., Grebel & Gallagher 2004).

The most definitive indicator of the presence of an ancient stellar population, which we take as one with an age comparable to the oldest Galactic halo globular clusters, is the observation of a faint main sequence turnoff luminosity. While with the *Hubble Space Telescope (HST)* it is possible with long total exposure times to reach fainter than the ancient main sequence turnoff luminosity in dwarf galaxies even at the edge of the Local Group (e.g. Cole et al. 2007; Bernard et al. 2009), it is frequently easier to characterise the presence of an ancient stellar population by confirming the existence of brighter markers. Foremost of these are blue horizontal branch (BHB) stars and RR Lyrae variables (RRLs), stars which are found only in ancient stellar populations². For example, we note that for the 14 Galactic globular clusters with $[\text{Fe}/\text{H}] < -1.4$ on the Carretta & Gratton (1997) scale that are classified as “old” in Marín-Franch et al. (2009), the median horizontal branch type (Lee et al. 1994) $(\text{B}-\text{R})/(\text{B}+\text{V}+\text{R})$ is 0.90, i.e., a horizontal branch morphology strongly dominated by BHB stars. Marín-Franch et al. (2009) show that the clusters in their “old” group have a small intrinsic age dispersion (~ 0.4 Gyr) and have ages consistent with formation in the epoch before reionization. We take the latter to be for $z > 6$, corresponding to age > 12.7 Gyr for the standard concordance cosmology (e.g., see Wright 2006). Further, the *youngest* star cluster known to contain RRLs is the SMC globular cluster NGC 121, which has an age of 11.2 ± 0.5 Gyr (Glatt et al. 2008) corresponding to a formation redshift $z \approx 3$, i.e., post reionization. However, many of the “old” clusters of Marín-Franch et al. (2009) also contain RRL stars.

Do dwarf galaxies beyond the Local Group contain ancient stars? While many color-magnitude diagrams (CMDs) exist for dwarf galaxies beyond the Local Group (e.g., Caldwell et al. 1998; Karachentsev et al. 2007; Dalcanton et al. 2009) the currently available observations generally do not reach faint enough to reveal the definitive markers of an ancient population. Such CMDs do reveal well developed metal-poor red giant branches (RGBs) but without using additional constraints, such as the presence, number and magnitude range of asymptotic giant branch (AGB) stars more luminous than the RGB tip, the RGB stars could be between ~ 2 and > 10 Gyr old. The

²We note in passing that for at least some of the recently discovered ultra-low luminosity dwarf galaxy companions to the Milky Way, measurement of the main sequence turnoff is only way to establish the presence of an ancient population as these systems lack sufficient stars to populate the core-helium burning (horizontal branch) phase of evolution.

question is not a trivial one as it involves the extent to which star formation occurs in low mass halos ($M \leq 10^8 M_\odot$) at the earliest times, i.e. before reionization, in environments different to that of the Local Group.

The nearest group of galaxies beyond the Local Group is the Sculptor Group, which is a loose collection of late-type spirals and dwarf galaxies spread out along the line-of-sight with distances ranging from ~ 1.5 to 5 Mpc (e.g., Jerjen et al. 1998; Karachentsev et al. 2003). There are 6 early-type dwarf systems identified as group members: the dS0/Im NGC 59 and the less luminous systems ESO294-010, ESO410-005, ESO540-030, ESO540-032 and Scl-dE1 (Scl22). Of these latter 5 systems, all except Scl-dE1 have detectable amounts of HI (Bouchard et al. 2005) and thus can be characterised as ‘transition dwarfs’, i.e., intermediate between gas-rich dIrr systems and gas-poor dE/dSph galaxies (e.g., Grebel et al. 2003). All five of these dwarfs are targets in our *HST* program; here we discuss first results for the two nearer systems ESO294-010 and ESO410-005. Using the apparent magnitudes listed in Bouchard et al. (2009) and the distance moduli derived below, these galaxies have $M_B \approx -11.0$ and -11.6 , respectively. As such they are comparable to Local Group dwarfs such as And I ($M_B \approx -11.2$) and Leo I (-11.1) (Mateo 1998).

2. Observations

Observations of ESO294-010 and ESO410-005 were taken in May 2006 with the Wide Field Channel (WFC) of the Advanced Camera for Surveys (ACS) on board *HST*. Both dwarfs fit comfortably within the WFC field-of-view. For ESO294-010 the total integration time was 13920 sec in the *F606W* filter (‘wide-*V*’) spread over 12 CR-split pairs of exposures, executed as 3 blocks of four. The interval between the first and last observations was 1.86 days. For the *F814W* filter ($\sim I$) the total integration time was 27840 sec over 24 CR-split pairs of exposures, executed as 6 blocks of four and spanning a range of 1.60 days. The individual blocks of four CR-split exposures were taken within a single visit using the so-called ‘parallelogram’ dither box pattern (Pavlovsky et al. 2004). For ESO410-005 the observations followed the same strategy, with total integration times of 13440 sec in *F606W* and 26880 sec in *F814W*. The *F606W* and *F814W* observations were both taken over a span of 4.54 days.

The primary images used for the analysis are the calibrated, geometrically corrected, and dither-combined *_drz* images that result from the standard ACS processing pipeline CALACS (Pavlovsky et al. 2004). These images were analyzed with the point-spread-function (PSF) fitting programs in the *DAOPHOT* and *ALLFRAME* packages (see Stetson 1987, 1994). In the first step all the images for both filters were registered and combined together into a single deep image. This image was used to generate the star list that functioned as input to *allframe*, which was applied to the three *_drz F606W* and six *_drz F814* images. The process was identical for both galaxies.

The resulting photometry sets were then combined, and objects with large χ , sharpness parameter or photometric error purged from the lists. To bring the photometry on to the ground-based

VI system we used the synthetic calibration equations of Sirianni et al. (2005). The aperture corrections from the *allframe* photometry to $0''.5$ aperture photometry were derived directly from the images, and we also applied the aperture corrections from $0''.5$ to infinite aperture (Sirianni et al. 2005). Charge Transfer Efficiency (CTE) corrections were investigated (see Riess & Mack 2004; Chiaberge et al. 2009) but were found to be smaller than 0.01 mag for almost all stars brighter than $I \approx 27.5$ mag and have been ignored. The final photometric catalogue contains 30411 sources in ESO294-010 and 30960 sources in ESO410-005 and the resulting CMDs are shown in the panels of Fig. 1.

3. Analysis

3.1. Color-magnitude diagrams

The CMDs of ESO294-010 and ESO410-005 shown in Fig. 1 are dominated by RGB stars. In both cases the I magnitude of the tip of the RGB, $I(\text{TRGB})$, is well defined. Application of standard Sobel filter techniques to the I -band luminosity function of the red giant branch yields $I(\text{TRGB}) = 22.45 \pm 0.07$ for ESO294-010 and 22.35 ± 0.07 for ESO410-005. Adopting reddenings $E(B - V)$ of 0.006 and 0.014 mag from Schlegel et al. (1998), respectively, and $M_I^{\text{TRGB}} = -4.05$ (e.g., Rizzi et al. 2007), then yields distances of 2.0 ± 0.1 Mpc and 1.9 ± 0.1 Mpc for ESO294-010 and ESO410-005, respectively. These values are in excellent accord with, for example, the distances tabulated in the ‘Extragalactic Distance Database’ compiled by Tully et al. (2009). In determining these distances we have ignored any reddening internal to the dwarf galaxies. This is justified as follows: using the Galactic neutral gas column density to reddening ratio given in, for example, Rachford et al. (2009) or Lockman & Condon (2005), and assuming neutral hydrogen column densities of $\sim 5 \times 10^{19} \text{ cm}^{-2}$ (Bouchard et al. 2005) in the dwarfs, the implied internal reddening is less than 0.01 mag. The actual value is likely to be even lower given the low metallicities of these systems compared to the Galaxy.

With the distance known we can then use a comparison of the red giant branch colors with either standard globular cluster giant branches (e.g., Da Costa & Armandroff 1990) or theoretical giant branches (e.g., VandenBerg et al. 2006) to estimate mean metallicities under the assumption that the stars on the RGB are predominantly old. This is reasonable given the relatively small number of (intermediate-age) AGB stars above the RGB tip in both galaxies (see Fig. 1). Applying the calibration given in Caldwell et al. (1998) for $(V - I)_{0,-3.5}$, the dereddened color of the giant branch at $M_I = -3.5$, which is based on the standard globular cluster giant branches of Da Costa & Armandroff (1990), the mean metallicities for ESO294-010 and ESO410-005 are $\langle [\text{Fe}/\text{H}] \rangle = -1.7 \pm 0.1$ and -1.8 ± 0.1 , respectively. These values agree well with the mean metallicities derived from using the 12 Gyr, $[\alpha/\text{Fe}] = 0$ theoretical giant branches of VandenBerg et al. (2006), which give $\langle [\text{Fe}/\text{H}] \rangle = -1.6 \pm 0.1$ and -1.7 ± 0.1 , respectively.

It is also apparent from the CMDs of Fig. 1 that both galaxies contain populations of young

blue main sequence stars, with that in ESO410-005 apparently relatively stronger than that of ESO294-010. The possible existence of young stars in these galaxies has been remarked on before (Karachentsev et al. 2000; Karachenstev et al. 2002). The existence of such stars is not surprising given that Bouchard et al. (2005) have demonstrated that ESO294-010 and ESO410-005 both contain modest amounts of neutral hydrogen gas, namely $3.0 \pm 0.3 \times 10^5 M_{\odot}$ for ESO294-010 and $7.3 \pm 1.5 \times 10^5 M_{\odot}$ for ESO410-005. A full population synthesis analysis of the CMDs and its implications for the star formation histories of these dwarf galaxies will be the subject of a future paper (Rejkuba et al., in preparation).

Within the context of the current paper, however, one of the most notable features of the CMDs of Fig. 1 is the clear presence of BHB stars in both galaxies. While the CMDs show that for both galaxies the majority of the core-helium burning stars lie in the red clump region, the existence of a sizeable population of BHB stars in these dwarf galaxies is undeniable. Populations of these ancient stars are seen in the CMDs of Local Group dwarfs, but the CMDs of Fig. 1 are the first direct demonstration of the existence of BHB stars in dwarf galaxies beyond the Local Group. We note in particular that the BHB populations of the Scl group dwarf galaxies in Fig. 1 appear relatively strong. For example, BHB stars are seemingly more frequent in the CMDs for these transition dwarfs than in the CMDs of the Cetus dSph (e.g., Bernard et al. 2009) and the transition dwarf LGS 3 (Miller et al. 2001), and are comparable to that for the Phoenix transition dwarf (Gallart et al. 2004). Detailed comparisons of horizontal branch structures, however, are postponed to a subsequent paper (Rejkuba et al., in preparation).

3.2. RR Lyrae candidates

The *allframe* photometry of the *F606W* and *F814W* image sets produces not only a combined magnitude for each object, but also a variability index, *var*, which is the ratio of the external to the internal errors. The external error is given by the frame-to-frame variation in the individual magnitude measurements while the internal error is dominated by the Poission photon noise of the star and sky scaled by the gain of the detector. Stars that truly vary over the epoch of the observations will have significant variability index values. In Fig. 1 we show as magenta points the 240 stars in the ESO294-010 photometry list and the 182 stars in the ESO410-005 list that satisfy $var(F606W) \geq 4.0$ (3 epochs) and/or $var(F814W) \geq 3.0$ (6 epochs) and which are brighter than $I \approx 27.2$ mag. Further, for both galaxies, all the candidates with $I \leq 26.1$ have been investigated using the *_crj* photometry (see below) and only those (the majority) exhibiting genuine periodic variability characteristics have been plotted.

Clearly most of the candidate variable stars are coincident with the horizontal branch in the galaxies. We note however, that identifying variables this way is unlikely to produce a complete set of variables, and that, because the individual *F606W* and *F814W* images were not obtained concurrently, the combined magnitude and colors from the *allframe* photometry will not represent the correct phase averaged magnitude and color of any variable star. This is the explanation for

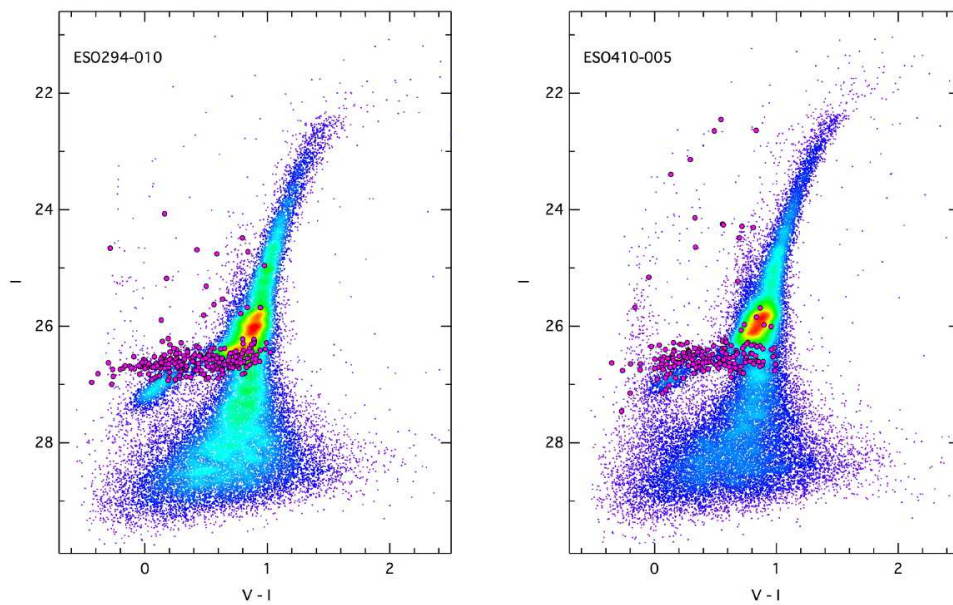


Fig. 1.— Color-Magnitude diagrams in the V and I bands for the Sculptor Group dwarf galaxies ESO294-010 and ESO410-005 derived from the *HST* ACS images. The color table used moves from purple to red to signify increasing density of points in the CMD. Over-plotted in magenta are the candidate variable stars for each dwarf, which are strongly concentrated to the horizontal branch.

the large spread in the colors of the candidate variables at the magnitude of the horizontal branch. It also means that the location of the candidate variables above the horizontal branch in Fig. 1 are unlikely to represent their true phase-averaged location in the CMD.

Nevertheless, the variable candidates at the magnitude of the horizontal branch are likely to be predominantly RRLs. The more luminous candidate variables, on the other hand, probably consist of a mixture of BL Her stars, Anomalous Cepheids, Pop II Cepheids, and short-period ($P \lesssim 2$ d) Classical Cepheids all of which are found in Local Group dwarf galaxies (e.g., Gallart et al. 2004; Pritzl et al. 2005; Bernard et al. 2009). Here we discuss only the RRL candidates, noting that the epoch span of the observations (1.9 d for ESO294-010, 4.5 d for ESO410-005) makes deriving light curves for all but the shorter period variables, such as RRLs, uncertain.

While the *var* index from 3 epochs in *F606W* and/or 6 epochs in *F814W* is clearly capable of identifying candidate variables, the corresponding *allframe* photometry does not provide enough information for any light curve analyses. Consequently, we have turned to the *_crj* data products from the ACS pipeline. These are the bias corrected, flat-fielded and cosmic-ray cleaned combinations of the two exposures from the CR-split pairs. These images have total exposure times of 1160 and 1120 sec for ESO294-010 and ESO 410-005, respectively, and allow 12 distinct *F606W* and 24 *F814W* magnitude estimates. The PSF-fitting photometry on these frames was carried out much in the same way as for the *_drz* data, including the derivation of the aperture corrections and the calibration to the VEGAMAG system (see Sirianni et al. 2005).

The sets of 12 *F606W* and 24 *F814W* magnitudes were then compiled for a small sample from the list of RRL candidates in each galaxy. The candidates chosen for follow-up were primarily selected from those with relatively large *var(F606W)* values, as the errors on the individual magnitudes are smaller for *F606W* and the amplitude of variation for an RRL is larger in this filter compared to *F814W*. This process necessarily biases against the selection of Type-c RRLs which have smaller amplitude variations than Type-ab stars. For each RRL candidate the sets of *F606W* and *F814W* magnitudes together with the mid-exposure Heliocentric Julian dates were fed separately into the phase dispersion minimization code (*pdm*) within IRAF. The output from the two data sets was then compared. The comparison generally permitted an estimate for the variability period that was consistent with both the *F606W* and *F814W* data. The *F606W* data were also analysed with the code provided by Layden in which χ^2 as a function of trial period is generated using a series of template light curves (see Layden 1998)³. The χ^2 minimum generally coincided with the period estimate from the *pdm* analysis to within 0.01 d. In Fig. 2 we show the *F606W* observations phased with the adopted period, and the best-fit Layden (1998) Type-ab RRL template light curve, for four example RRL candidates in ESO294-010 (left column) and in ESO410-005 (right column). The phased *F814W* data for these stars are not shown but are con-

³Strictly the template light curves are in the *V*-band, not *F606W*. However, using the transformation equations of Sirianni et al. (2005) and a typical (*V* – *I*) color range of ~ 0.4 mag during its cycle, the maximum change in *V*–*F606W* for a RRL is < 0.10 mag, and has been neglected.

sistent with the periods adopted from the $F606W$ data. The periods found lie in the range 0.51 – 0.64 d and the amplitudes are of order 1 magnitude consistent with the properties of Type-ab variables. Further, the mean magnitudes of the stars are consistent, assuming the distance moduli calculated from the I(TRGB) values, with absolute magnitudes $M_V \approx +0.6$. *The stars are thus clearly RRL variables, the first such stars to be characterised beyond the Local Group.*

4. Discussion

Just as the existence of BHB and RRL stars in the old globular clusters of our Galaxy requires significant star formation during the pre-reionization epoch within the dark matter halos that merged to form the Milky Way, the existence of BHB stars and RRL variables in the Sculptor Group dwarf galaxies ESO294-010 and ESO410-005 suggests that star formation occurred at the earliest epochs in these systems as well, much as it also did in the Local Group dwarfs. The Sculptor Group, however, is a notably different environment from the Local Group – it is much less dense and lacks dominant galaxies in the way that the Local Group is dominated by M31 and the Galaxy. Indeed there is little evidence for much dynamical evolution in the group; Bland-Hawthorn et al. (2005) have shown, for example, that the outer disk of the late-type spiral NGC 300 continues for an unprecedented 10 radial scale lengths with no sign of any disturbance or truncation, in marked contrast to the situation for M31 (e.g. Ibata et al. 2007) in the Local Group. Thus from a cosmological point-of-view our results suggest that gas can condense and form stars in low mass halos at the earliest epochs even in relatively low density environments. Further, given the substantial number of red clump stars in the CMDs, which are likely to have ages less than 10 Gyr, it appears that the subsequent star formation in these dwarfs was not obviously affected by reionization. This is consistent with the observational results for Local Group dwarfs (Grebel & Gallagher 2004) but inconsistent with theoretical results that predict post-reionization star formation in dwarf galaxies should be strongly suppressed (e.g., Babul & Rees 1992; Bullock et al. 2000; Ricotti & Gnedin 2005). Clearly as we learn more of the star formation histories of dwarf galaxies in environments beyond the Local Group we will be able to better constrain the role of these cosmological processes.

MR would like to acknowledge support from an ESO DGDF grant and from the Australian National University that enabled a productive visit to Mt Stromlo Observatory.

Facilities: HST

REFERENCES

- Baade, W., & Hubble, E. 1939, PASP, 51, 40
 Babul, A., & Rees, M. J. 1992, MNRAS, 255, 346

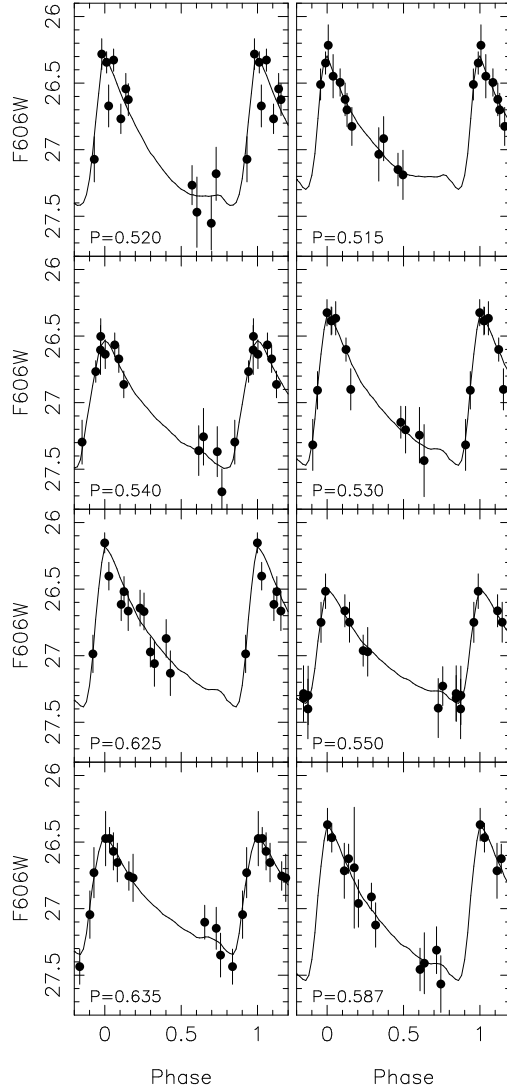


Fig. 2.— $F606W$ ($\sim V$) light curves for example RR Lyrae stars in ESO294-010 (left column) and in ESO410-005 (right column). The solid curves are the best fit to the observations using the Type-ab V -band template light curves from Layden (1998) for the period (in days) shown in each panel. There are 12 independent brightness measures for each star.

- Bernard, E. J., et al. 2009, *ApJ*, 699, 1742
- Bland-Hawthorn, J., Vlajić, M., Freeman, K. C., & Draine, B. T. 2005, *ApJ*, 629, 239
- Bouchard, A., Jerjen, H., Da Costa, G. S., & Ott, J. 2005, *AJ*, 130, 2058
- Bouchard, A., Da Costa, G. S., & Jerjen, H. 2009, *AJ*, 137, 3038
- Bullock, J. S., Kravtsov, A. V., & Weinberg, D. H. 2000, *ApJ*, 539, 517
- Caldwell, N., Armandroff, T. E., Da Costa, G. S., & Seitzer, P. 1998, *AJ*, 115, 535
- Carretta, E., & Gattton, R. G. 1997, *A&AS*, 121, 95
- Chiaberge, M., et al. 2009, Instrument Science Report ACS 2009-01, (Baltimore: STScI)
- Cole, A. A., et al. 2007, *ApJ*, 659, L17
- Da Costa, G. S., & Armandroff, T. E. 1990, *AJ*, 100, 162
- Dalcanton, J. J., et al. 2009, *ApJS*, 183, 67
- Gallart, C., Aparicio, A., Freedman, W. L., Madore, B. F., Martínez-Delgado, D., & Stetson, P. B. 2004, *AJ*, 127, 1486
- Glatt, K. et al. 2008, *AJ*, 135, 1106
- Grebel, E. K., & Gallagher, J. S. III 2004, *ApJ*, 610, L89
- Grebel, E. K., Gallagher, J. S. III, & Harbeck, D., 2003, *AJ*, 125, 1926
- Ibata R., Martin, N. F., Irwin, M., Chapman, S., Ferguson, A. M. N., Lewis, G. F., & McConnachie, A. W. 2007, *ApJ*, 671, 1591
- Jerjen, H., Freeman, K. C., & Binggeli, B. 1998, *AJ*, 116, 2873
- Karachentsev, I. D., et al. 2000, *ApJ*, 542, 128
- Karachentsev, I. D., et al. 2002, *A&A*, 389, 812
- Karachentsev, I. D., et al. 2003, *A&A*, 404, 93
- Karachentsev, I. D., et al. 2007, *AJ*, 133, 504
- Layden, A. C. 1998, *AJ*, 115, 193
- Lee, Y.-W., Demarque, P., & Zinn, R. 1994, *ApJ*, 423, 248
- Lockman, F. J., & Condon, J. J. 2005, *AJ*, 129, 1968

- Marín-Franch, A., et al. 2009, *ApJ*, 694, 1498
- Mateo, M. 1998, *ARA&A*, 36, 435
- Miller, B. W., Dolphin, A. E., Lee, M. G., Kim, S. C., & Hodge, P. 2001, *ApJ*, 562, 713
- Pavlovsky, C., et al. 2004, *ACS Data Handbook*, Version 3.0, (Baltimore: STScI)
- Pritzl, B. J., Armandroff, T. E., Jacoby, G. H., & Da Costa, G. S. 2005, *AJ*, 129, 2232
- Rachford, B. L., et al. 2009, *ApJS*, 180, 125
- Ricotti, M., & Gnedin, N. Y. 2005, *ApJ*, 629, 259
- Riess, A., & Mack, J. 2004, *Instrument Science Report ACS 2004-006*, (Baltimore: STScI)
- Rizzi, L., Tully, R.B., Makarov, D., Markarova, L., Dolphin, A.E., Sakai, S., & Shaya, E. 2007, *ApJ*, 661, 815
- Schlegel, D. J., Finkbeiner, D. P., & Davis, M. 1998, *ApJ*, 500, 525
- Shapley, H. 1938, *Havard College Obs. Bull.*, 908, 1
- Sirianni, M., et al. 2005, *PASP*, 117, 1049
- Stetson, P.B. 1987, *PASP*, 99, 191
- Stetson, P.B. 1994, *PASP*, 106, 250
- Tully, R. B., Rizzi, L., Shaya, E. J., Courtois, H. M., Makarov, D. I., & Jacobs, B. A. 2009, *AJ*, 138, 323
- Vandenberg, D. A., Bergbusch, P. A., & Dowler, P. D. 2006, *ApJS*, 162, 375
- Wright, E. L. 2006, *PASP*, 118, 1711